Research Article

Received: 4 August 2014 Revised: 2 October 2014 Accepted article published: 8 October 2014 Published online in Wiley Online Library: 10 November 2014

(wileyonlinelibrary.com) DOI 10.1002/jctb.4567

Electrochemical conversion of sulfur dioxide with a rotating cylinder electrode working as anode or cathode

Juan P. Fornés, Gabriel A. González and José M. Bisang*

Abstract

BACKGROUND: A batch electrochemical reactor with a rotating cylinder electrode is analysed for the transformation of sulfur dioxide into either sulfuric acid or colloidal sulfur.

RESULTS: Potentiostatic experiments carried out at 30 °C and 500 rpm with 5 g L^{-1} SO_2 in 0.5 mol L^{-1} H_2SO_4 conclude that −0.7 V, against SCE, represents an appropriate potential for the sulfur production at a 316 L stainless steel cathode. The figures of merit were: 0.15 kg m^{-3} h^{-1} space time yield and 39.7 kWh kg^{-1} for specific energy consumption. Galvanostatic experiments at 30 °C and 1000 rpm with three-dimensional electrodes identify graphite felt as a promising anodic material. Using a gas phase of 5% SO_2 in nitrogen and 0.5 mol L^{-1} H_2SO_4 as supporting electrolyte, a macrokinetic current density of 100 mA cm^{-2} represents an appropriate value, being the space time yield 7.58 kg m^{-3} h^{-1} with 2.86 kWh kg^{-1} specific energy consumption.

CONCLUSION: An electrochemical reactor with a rotating cylinder electrode showed a good performance for the production of colloidal sulfur. Sulfur dioxide was also converted into sulfuric acid including a separator in a reactor with a three-dimensional rotating cylinder anode and co-current gas and liquid flows.

Keywords: sulfur dioxide; electrochemical reactor; rotating cylinder electrode; sulfur production; sulfuric acid production

INTRODUCTION

Sulfur dioxide is generated during the burning of fossil fuels for energy production and in other manufacturing processes such as the smelting of metals, sulfuric acid production and the synthesis of chromic sulfate as a tanning agent for leather. Sulfur dioxide presents deleterious effects on the environment and several technologies are proposed for its abatement.[1,2] Stimulated by the increasing importance of sulfur dioxide pollution control, many attempts have been made to develop electrochemical processes for its removal, which are mainly focussed on flue gas desulfurization by anodic oxidation.[3–5] Recently, electrochemical processes for gaseous sulfur dioxide removal were reviewed by Bakir Öğütveren.[6] Scant attention has been paid to its removal by cathodic reduction. Thus, Oloman[7] and Oloman and co-workers[8] analyzed the electrosynthesis of dithionite and Scott *et al.*[9,10] reported on its reduction to elemental sulfur. Likewise, the oxidation of sulfur dioxide to sulfuric acid is also recognized as an appropriate anodic reaction in the hybrid processes for hydrogen production,[11,12] in which different materials were examined to determine the best performance for the anode. Sulfur dioxide oxidation was also proposed as an alternative reaction to oxygen evolution for the electro-winning of metals in order to diminish the cell voltage.[13]

This paper analyses the best conditions for the electrochemical transformation of sulfur dioxide using both rotating disc and cylinder electrodes, in which the contaminant is transformed into either sulfuric acid or elemental sulfur.

FUNDAMENTAL STUDIES WITH A ROTATING DISC ELECTRODE

Experimental details

A rotating disc electrode was used to obtain the polarization curves because this electrochemical system presents well-defined hydrodynamic conditions and the mass transport characteristics are well known. The working electrode consisted of a disc with a 3 mm diameter embedded in a Teflon cylinder with a 10 mm diameter. Discs made of glassy carbon, copper, lead and 316 L stainless steel were used as working electrode. A platinum wire with a 1 mm diameter and 100 mm long was used as counter electrode. A saturated calomel electrode, SCE, served as reference and the potentials are referred to this electrode.

* *Correspondence to: José M. Bisang, Programa de Electroquímica Aplicada e Ingeniería Electroquímica (PRELINE), Facultad de Ingeniería Química, Universidad Nacional del Litoral, Santiago del Estero 2829, S3000AOM Santa Fe, Argentina, E-mail: jbisang@fiq.unl.edu.ar*

Correction Note: This article was first published online on the 10th of November 2014. It was corrected on the 19th of August 2015. In the original publication the last compound of equation 5 reads '$3H_2O$' when it should have read '$3H_2SO_4$'. The error has been corrected in this version of the article.

Programa de Electroquímica Aplicada e Ingeniería Electroquímica (PRELINE), Facultad de Ingeniería Química, Universidad Nacional del Litoral, Santiago del Estero 2829, S3000AOM, OM, Santa Fe, Argentina

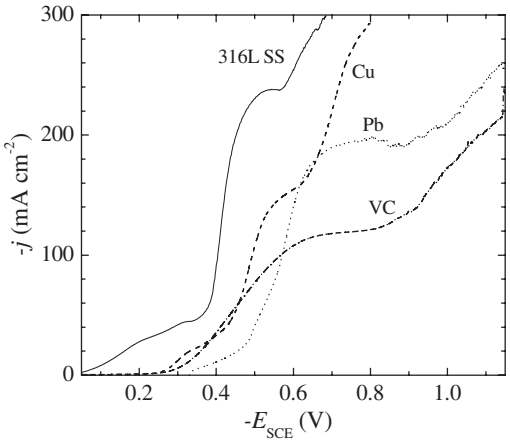

Figure 1. Current density as a function of the electrode potential for sulfur dioxide reduction at different electrode materials. 5 g L^{-1} SO_2 in 0.5 mol L^{-1} H_2SO_4 as supporting electrolyte. $\omega = 1000$ rpm. $T = 30\,°C$. Potential sweep rate: 2 mV s^{-1}.

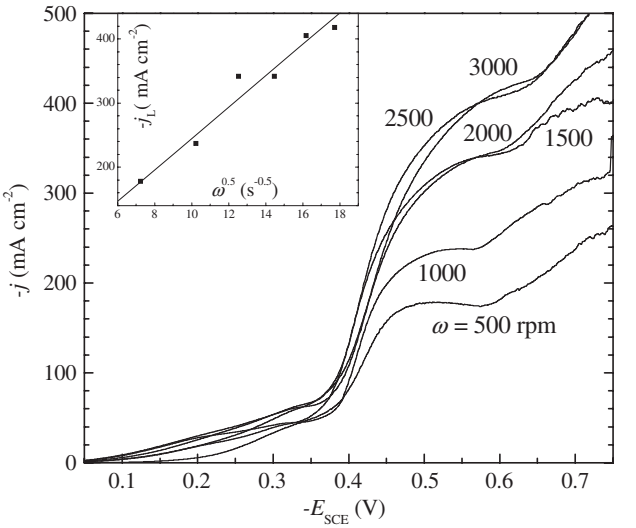

Figure 2. Current density as a function of the electrode potential for sulfur dioxide reduction at different rotation speeds. Cathode: 316 L stainless steel. 5 g L^{-1} SO_2 in 0.5 mol L^{-1} H_2SO_4 as supporting electrolyte. $T = 30\,°C$. Inset: Levich plot. j_L, limiting current density. Potential sweep rate: 2 mV s^{-1}.

The surface of the working electrode was polished to a bright mirror finish with slurry of 0.3 µm alumina powder and copiously washed with distilled water. Experiments were performed using a solution of 5 g L^{-1} SO_2 in 0.5 mol L^{-1} H_2SO_4 as supporting electrolyte, prepared dissolving sodium sulfite in an aqueous solution of sulfuric acid to achieve the above concentrations. The experiments were carried out potentiostatically under a slow potentiodynamic sweep rate of 2 mV s^{-1} to obtain steady-state polarization curves. The temperature and the rotation speed were 30 °C and 1000 rpm, respectively, unless otherwise indicated.

Results and discussion

Figure 1 shows cathodic polarization curves for the different electrode materials. In all cases the current increases when the electrode potential decreases, approaching a limiting value, which can be attributed to the reduction of sulfur dioxide. However, the limiting current density depends on the electrode material showing that the products of the sulfur dioxide reduction mask the electrode surface, or that different cathodic reactions can occur depending on the material. At more negative cathodic potentials, the current increases due to hydrogen evolution. Then, it is observed that the reduction of sulfur dioxide takes place earlier than hydrogen evolution in all materials. From a catalytic point of view, it can be inferred that 316 L stainless steel shows the best performance for sulfur dioxide reduction in acid solutions and −0.5 V can be recognized as an appropriate cathodic potential to achieve limiting current conditions for the main reaction without hydrogen evolution as a side reaction. For the reduction of sulfur dioxide in acid media the following reactions can be proposed:

$$SO_2 + 4H^+ + 4e^- \rightarrow S + 2H_2O \quad (1)$$

and

$$SO_2 + 6H^+ + 6e^- \rightarrow H_2S + 2H_2O \quad (2)$$

Figure 2 shows polarization curves for the sulfur dioxide reduction at different rotation speeds, ω, and the inset represents the Levich plot. The diffusion coefficient of sulfur dioxide, obtained from the slope of the line, is 1.53×10^{-9} m^2 s^{-1}, which agrees with the literature value.[14] In these calculations 4 was assumed as the number of exchanged electrons per sulfur dioxide molecule and 1.07×10^{-6} m^2 s^{-1} for the kinematic viscosity of the solution. The high current density and the narrow range of potentials where the reduction of sulfur dioxide takes place under limiting current conditions suggest that it is unnecessary to use a three-dimensional cathode to carry out this reaction.

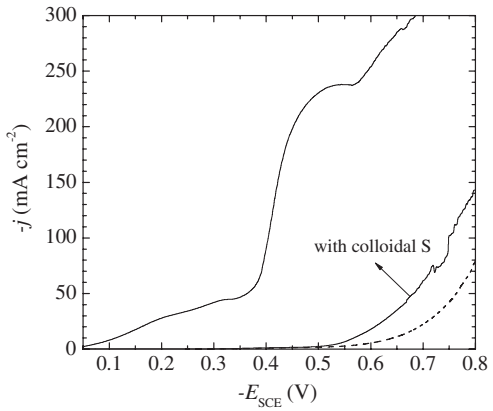

Figure 3. Current density as a function of the electrode potential for sulfur dioxide reduction with and without the presence of colloidal sulfur. Cathode: 316 L stainless steel. 5 g L^{-1} SO_2 in 0.5 mol L^{-1} H_2SO_4 as supporting electrolyte. $\omega = 1000$ rpm. $T = 30\,°C$. Potential sweep rate: 2 mV s^{-1}. Dashed line: supporting electrolyte.

Figure 3 reports on the influence of the presence of colloidal sulfur in the kinetics of the sulfur dioxide reduction, where it can be observed that the electrode is deactivated, because elemental sulfur probably masks the electrode surface.

The polarization curves for the sulfur dioxide oxidation at a glassy carbon electrode with and without the presence of colloidal sulfur are shown in Fig. 4. It can be detected that the current density increases with the anodic potential achieving a limiting current, which can be attributed to the following reaction:

$$SO_2 + 2H_2O \rightarrow HSO_4^- + 3H^+ + 2e^- \quad (3)$$

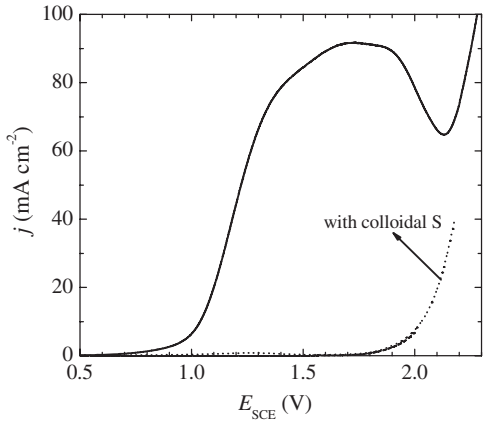

Figure 4. Current density as a function of the electrode potential for sulfur dioxide oxidation at glassy carbon. 5 g L^{-1} SO_2 in 0.5 mol L^{-1} H_2SO_4 as supporting electrolyte. $\omega = 1000$ rpm. $T = 30\,^{\circ}C$. Potential sweep rate: 2 mV s^{-1}. Dashed line: supporting electrolyte. Dotted line: in presence of colloidal sulfur.

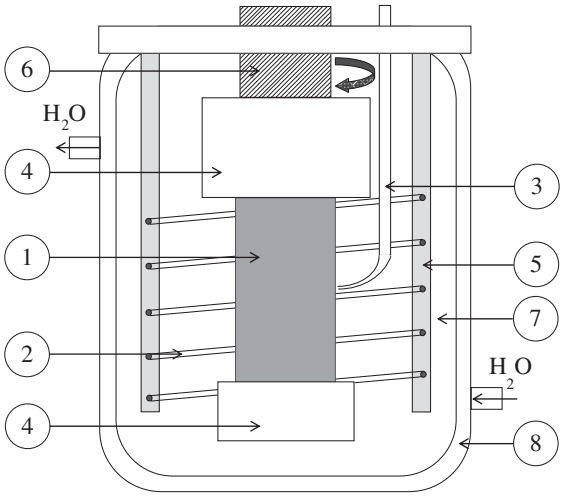

Figure 5. Schematic representation of the electrochemical reactor with a cylindrical rotating electrode. 1, Working electrode; 2, counter electrode; 3, Luggin capillary; 4, Teflon sleeve; 5, counter-electrode support; 6, electrode shaft; 7, electrolyte container; 8, heating jacket.

The increase in current at more anodic potentials is due to oxygen evolution as it is corroborated by the dashed line obtained with the supporting electrolyte. The dotted curve shows the behavior of the system in the presence of colloidal sulfur, which completely inhibits the oxidation of sulfur dioxide. From Fig. 4 it can be concluded that a potential of 1.5 V against a saturated calomel electrode is an appropriate anodic potential to work close to limiting current conditions without oxygen evolution, and in industrial practice it is necessary to use a separator between the anodic and cathodic compartments in order to hinder the deactivation of the anode by the sulfur cathodically produced. Comparing Fig. 3 and Fig. 4 it can be observed that the limiting current for sulfur dioxide reduction is higher than twice the limiting value for its oxidation, which suggests that the cathodic reduction of sulfur dioxide must involve a reaction with a number of electrons higher than four as can be inferred from the combination of reactions (1) and (2), according to:

$$\left(1+\frac{\beta_c}{2}\right)SO_2 + 6H^+ + 6e^- \rightarrow \frac{3\beta_c}{2}S + \left(1-\beta_c\right)H_2S + \left(2+\beta_c\right)H_2O \quad (4)$$

where β_c is the current efficiency for the sulfur production. Adding Eqns (3) and (4) yields:

$$\left(4+\frac{\beta_c}{2}\right)SO_2 + \left(4-\beta_c\right)H_2O \xrightarrow{6F} \frac{3\beta_c}{2}S + \left(1-\beta_c\right)H_2S + 3\,H_2SO_4 \quad (5)$$

which represents the overall reaction for the electrochemical reactor, being F the Faraday constant. Equation (5) also shows that the cathodic reactions do not alter the pH of the solution.

EXPERIMENTS WITH A CYLINDRICAL BATCH REACTOR

Reduction of sulfur dioxide in an undivided reactor

Long-term experiments were performed in a batch reactor with a 95 mm internal diameter and 140 mm high using a rotating cylinder as working electrode. The reactor was thermostated using a heating jacket. The complete experimental arrangement is schematically depicted in Fig. 5. The working electrode was a 316 L stainless steel cylinder, 22 mm diameter and 39 mm long, bounded by Teflon sleeves, 30 mm diameter in the lower part and 37.5 mm diameter in the upper part. The sleeves protrude from the cathode and form a right angle with it, thereby preventing a sharp increase in the current near the edges, which homogenizes the current distribution along the electrode length. As counter electrode a concentric helical platinum wire, 1 mm diameter and 100 cm long, was used with a 19 mm inter-electrode gap. A saturated calomel electrode connected to a Luggin capillary located in the middle region at the surface of the working electrode was used as reference. The upper end of the cylindrical rotating electrode was attached to the motor shaft. Experiments were performed using a solution of 5 g L^{-1} SO_2 in 0.5 mol L^{-1} H_2SO_4 as supporting electrolyte prepared following the procedure stated above. The experiments were performed potentiostatically at 30 °C with a solution volume of 0.75 L. Both cell voltage and current were measured. At the end of the experiment the pH of the solution was adjusted to 7 and the sulfur was precipitated. The solution was taken out and the amount of elemental sulfur in the precipitate was determined with the method described by Morris *et al.*[15]

Figure 6 shows the current density for sulfur dioxide reduction as a function of time at different cathodic potentials. These long-term experiments show a marked decrease in current with time, which corroborates that the cathode is deactivated. Two experiments, at −0.45 V and at −0.5 V, were carried out with a scrapper to remove the sulfur formed at the cathode. A lower decrease in the current can be observed at the beginning of the experiments, but after two hours the current approaches the value obtained without the scrapper. Experiments performed at potentials more negative than −0.5 V, where hydrogen evolution is possible as a side reaction, show also a decrease in the current with electrolysis time, but at high times the current approaches a constant value larger than those obtained at less negative potentials. The inset in Fig. 6 reports on current efficiency for sulfur production as a function of the cathodic potential. It can be observed that the current efficiency is approximately 50% for potentials where hydrogen evolution is not possible. Thus, in this potential range alternative reactions to the sulfur production must take place. The reduction of sulfur dioxide with the formation of sodium dithionite or thiosulfate can be disregarded because the reddish–brown

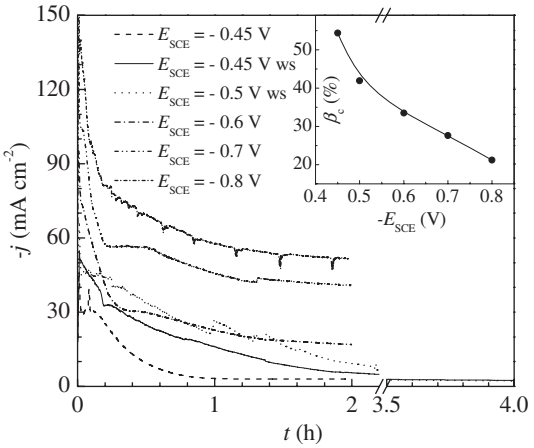

Figure 6. Current density as a function of time at different cathodic potentials for sulfur dioxide reduction at a stainless steel rotating cylinder electrode. 5 g L^{-1} SO_2 in 0.5 mol L^{-1} H_2SO_4 as supporting electrolyte. $\omega = 500$ rpm. $T = 30\,^{\circ}C$. Anode: Pt. Inset: cathodic current efficiency as a function of the potential. ws: with scrapper.

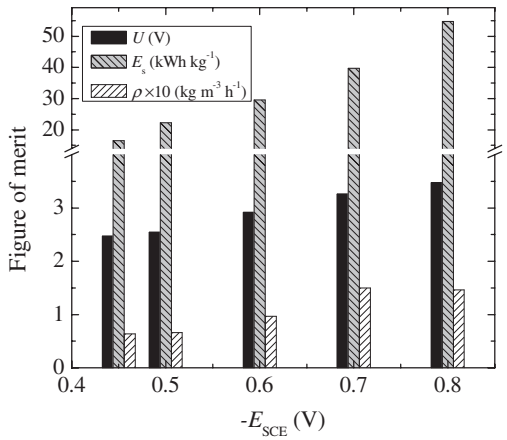

Figure 7. Figures of merit for the sulfur production at a stainless steel rotating cylinder electrode as a function of the cathodic potential. 5 g L^{-1} SO_2 in 0.5 mol L^{-1} H_2SO_4 as supporting electrolyte. $\omega = 500$ rpm. $T = 30\,^{\circ}C$. Anode: Pt. U, cell voltage; E_s, specific energy consumption; ρ, space time yield.

colour, characteristic of the former,[7,8] was not observed and the latter is unstable in acid media.[16] However, sulfide was detected in the solution by an additional qualitative analysis using the spot test with iodine and sodium azide.[17] Then, the reduction of sulfur dioxide to hydrogen sulfide, reaction (2), can be proposed as occurring simultaneously with sulfur production, reaction (1). At potentials more negative than −0.5 V hydrogen evolution also takes place and the current efficiency for sulfur production diminishes. Thus, hydrogen evolution can be recognized as beneficial for the removal of the sulfur layer covering the cathode, but it shows as a drawback the decrease in the current efficiency for sulfur production. To elucidate the more appropriate value for the cathodic potential, Fig. 7 shows the figures of merit of the reactor for the production of colloidal sulfur. An increase in both cell voltage and specific energy consumption is observed when the cathodic potential becomes more negative. The high specific energy consumption is a consequence of three factors: (1) the high number of electrons required for the cathodic reaction, (2) the low current efficiency and (3) the high anodic potential because of the

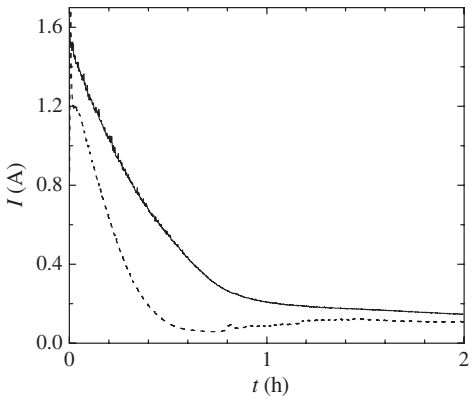

Figure 8. Current as a function of time for an undivided reactor with rotating cylinder electrodes. 5 g L^{-1} SO_2 in 0.5 mol L^{-1} H_2SO_4 as supporting electrolyte. $\omega = 500$ rpm. $T = 30\,^{\circ}C$. Full line: graphite rotating cylinder electrode at 1.5 V with a 316 L stainless steel cathode. Dashed line: 316 L stainless steel rotating cylinder electrode at −0.45 V with a graphite anode.

presence of colloidal sulfur. The space time yield increases as the cathodic potential is more negative allowing hydrogen production. The gas evolution removes the layer of sulfur deposited at the cathode and at the same time promotes the mass-transfer of sulfur dioxide, called bubble induced convection; both actions improve the formation of elemental sulfur. However, for cathodic potentials more negative than −0.7 V hydrogen evolution predominates over sulfur production and the space time yield diminishes. Then, from Fig. 7 it can be recognized that −0.7 V is an optimal value for the cathodic potential, for which the figures of merit of the reactor are: 3.26 V average cell voltage, 0.15 kg m^{-3} h^{-1} space time yield and 39.7 kWh kg^{-1} for specific energy consumption.

Oxidation of sulfur dioxide in an undivided reactor

The reactor depicted in Fig. 5 was also used for long-term experiments concerning the oxidation of sulfur dioxide. The working electrode was a graphite cylinder, grade 6503 Carbone Lorraine (Mersen, Buenos Aires, Argentina), 22 mm diameter and 39 mm long. As counter electrode a concentric helical 316 L stainless steel wire, 2.25 mm diameter and 160 cm long, was used with a 21 mm inter-electrode gap. The full line in Fig. 8 reports on the current as a function of time for a typical experiment at an anodic potential of 1.5 V in a solution of 5 g L^{-1} SO_2 in 0.5 mol L^{-1} H_2SO_4 as supporting electrolyte. Moreover, the composition of the electrolyte was determined at the end of the experiment by inductively coupled plasma spectroscopy given: 352 ppm Fe, 81 ppm Ni and 159 ppm Cr, which were produced by the corrosion of the counter electrode contaminating the electrolyte. Likewise, as a comparison, in Fig. 8 is also included, as dashed line, the behavior of the reactor with a 316 L stainless steel cylindrical rotating electrode potentiostatically controlled at −0.45 V. Three bars of graphite were used as counter electrode, placed symmetrically around the rotating electrode, with a 19 mm inter-electrode gap. A pronounced decrease in the current with time is observed in both experiments demonstrating that a divided electrochemical reactor is necessary for the production of sulfuric acid, which corroborates the results obtained with the rotating disc electrode.

Oxidation of sulfur dioxide in a divided reactor with a three-dimensional anode

The electrode arrangement is shown in Fig. 9. The working electrode was formed by a graphite cylinder, Carbone Lorraine grade

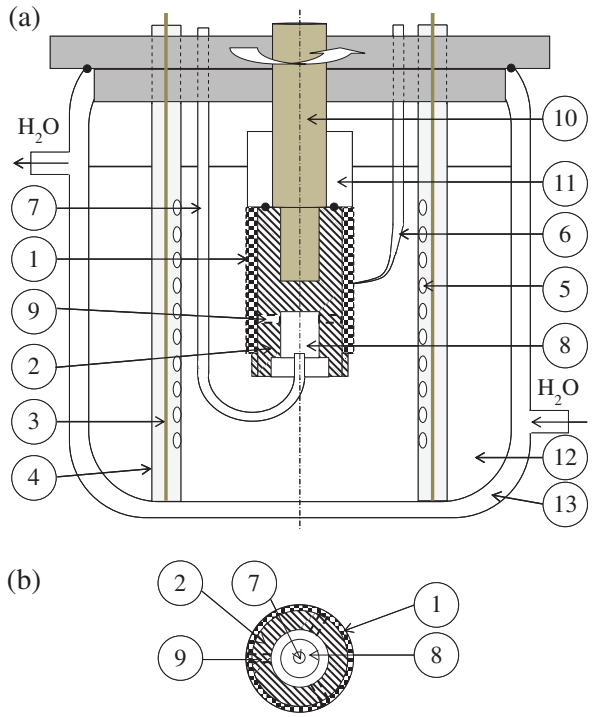

Figure 9. (a) Schematic representation of the electrochemical reactor with a three-dimensional anode and (b) bottom view of the working electrode. 1, Three-dimensional structure; 2, graphite support; 3, counter electrode; 4, anodic compartment; 5, window for the separator; 6, Luggin capillary; 7, oxygen feeder; 8, oxygen chamber; 9, channels for oxygen distribution; 10, electrode shaft; 11, Teflon cylinder; 12, electrolyte container; 13, heating jacket.

6503 E, 22 mm diameter and 44 mm long, which supports the three-dimensional electrodes made of either reticulated vitreous carbon or graphite felt, both supplied by The Electrosynthesis Co., Inc. (Lancaster, NY, USA). In the first case, three ring-shaped discs, 22 mm internal diameter, 42 mm external diameter and 12.7 mm high were placed on the cylindrical graphite support to form the three-dimensional electrode. In the second case, a sheet of graphite felt was wound around the cylindrical graphite support and maintained in position by a helical plastic outer support. In both cases the three-dimensional material was fixed to the support by graphite paint, which enhances the electrode conductivity. In the experiments GF-S4 graphite felt, fine pressed felt 0.3 mm, and reticulated vitreous carbon, RVC 100 ppi, were used. The bed depth of the three-dimensional structures in the direction of the current flow, 10 mm for RVC and 0.3 mm for GF-S4, ensures that the whole bed was working under limiting current conditions.[18]

A mix of 5% SO_2 and 95% N_2 was fed at 0.1 MPa into a chamber inside the graphite cylinder, via a port located at its lower end, and flowed through the three-dimensional electrode via three radial channels symmetrically drilled in the support. Figure 9b shows a bottom view of the working electrode. Thus, a co-current radial flow of the liquid and gas phases is induced by the centrifugal force of the rotation, resulting in appropriate intermixing between them. Two advantages can be recognized for this flow arrangement: (1) the reactant is fed in the same place where it is consumed allowing the sulfur dioxide concentration to remain constant and (2) the structure of the three-dimensional anode is also used as a gas distributor. The gas volumetric flow rate was set in the range between 4.17×10^{-6} m^3 s^{-1} and 13.89×10^{-6} m^3 s^{-1}, under

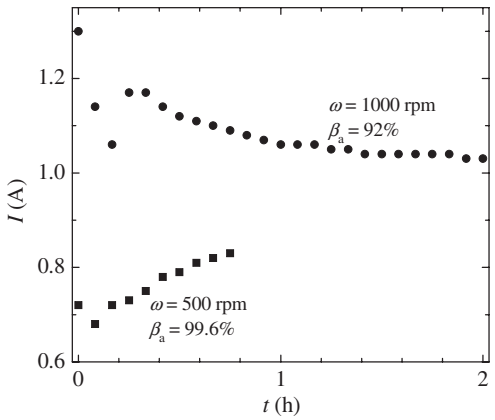

Figure 10. Current as a function of time for the graphite support without the three-dimensional electrode. 5% SO_2 in nitrogen with 0.5 mol L^{-1} H_2SO_4 as supporting electrolyte. $E_{SCE} = 1.5$ V. $T = 30$ °C. $Q = 4.17 \times 10^{-6}$ m^3 s^{-1}.

ambient conditions, and it was also bubbled through the solution for 1 h before the experiment to ensure that the electrolyte was saturated with sulfur dioxide. In a previous work,[19] the liquid volumetric flow rate at 1000 rpm rotation speed was calculated as 1×10^{-3} m^3 s^{-1}, which is higher than the gas volumetric flow rate. Then, it is expected that the hydrodynamic behavior of the reactor, the mass-transfer and the ohmic drop in the solution phase will be hardly influenced by the gas phase. Three platinum wires, 1.0 mm diameter and 120 mm long, were used as cathodes. Each cathode was separated from the anodic compartment by a cylindrical separator made of a double layer of microporous PVC sheet, forming three cathodic compartments, 22 mm external diameter, symmetrically placed around the rotating electrode. The gap between the external surface of the graphite felt working electrode and the separator was 20 mm. The working electrode and the counter electrode were concentric. Then, taking into account that the reaction is under mass-transfer control, a uniform tertiary current distribution can be assumed. The anode potential was measured against a saturated calomel electrode connected to a Luggin capillary located in the middle region at the external surface of the working electrode.

The experiments were performed galvanostatically at 30 °C in 0.5 mol L^{-1} H_2SO_4 as the supporting electrolyte. The cell voltage and the anodic potential were recorded along time. At the end of the experiment a sample of the solution was taken from the anodic compartment and the sulfuric acid concentration was volumetrically determined.[20]

Figure 10 shows the current as a function of time for the graphite support without the three-dimensional electrode at two rotation speeds, where the anode potential was maintained at 1.5 V against saturated calomel electrode. The current efficiencies were 99.6% and 92.0%, at 500 rpm and 1000 rpm, respectively, which corroborates that the main anodic reaction is the sulfur dioxide oxidation.

The current efficiency as a function of the current is reported in Fig. 11 for RVC 100 and GF-S4. The graphite felt shows a better performance than RVC 100 having high current efficiencies at high values of current. The anode potential as a function of time for the graphite felt electrode under the conditions reported in Fig. 11 is given in Fig. 12. Taking into account Fig. 12, it can be observed that at currents higher than 4 A the anode potential exceeds 1.5 V allowing oxygen evolution as a secondary reaction, which explains the low values of current efficiency when the current

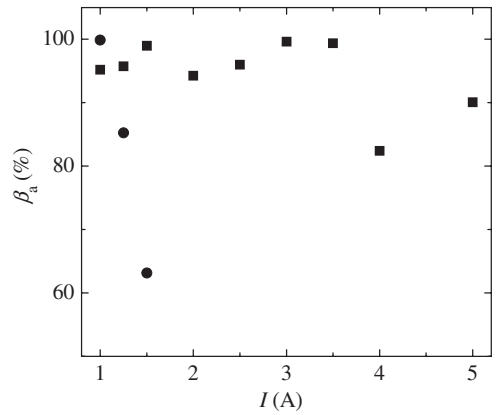

Figure 11. Current efficiency for sulfur dioxide oxidation as a function of the current. (■): GF-S4. (●): RVC 100 ppi. 5% SO_2 in nitrogen with 0.5 mol L^{-1} H_2SO_4 as the supporting electrolyte. $t = 2$ h. $\omega = 1000$ rpm. $T = 30$ °C.

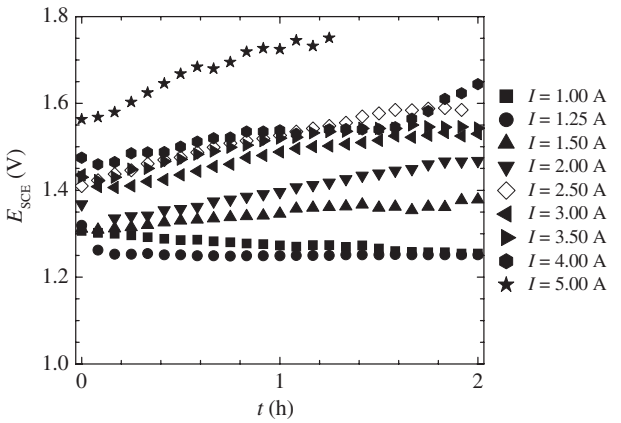

Figure 12. Anode potential as a function of time for GF-S4 as electrode material. 5% SO_2 in nitrogen with 0.5 mol L^{-1} H_2SO_4 as supporting electrolyte. $t = 2$ h. $\omega = 1000$ rpm. $T = 30$ °C.

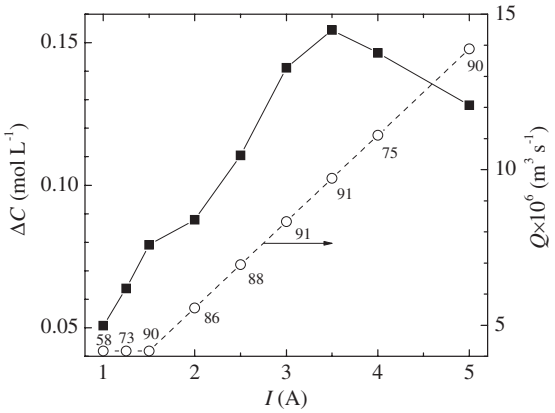

Figure 13. Change of concentration in sulfuric acid as a function of time for GF-S4 as anode material. (○) and dashed line: gas volumetric flow rate bubbled in the reactor, the number at each point represents the conversion of sulfur dioxide. 5% SO_2 in nitrogen with 0.5 mol L^{-1} H_2SO_4 as supporting electrolyte. $t = 2$ h. $\omega = 1000$ rpm. $T = 30$ °C.

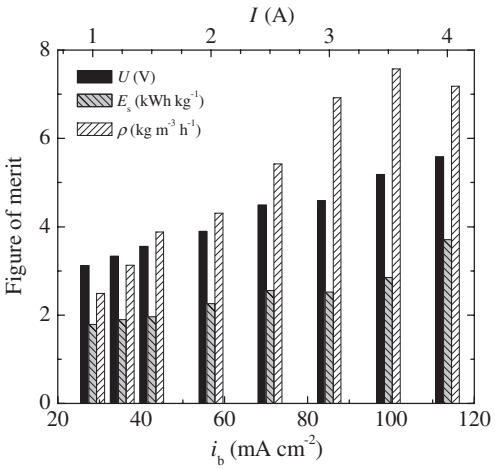

Figure 14. Figures of merit for the sulfuric acid production as a function of the macrokinetic current density. GF-S4 as anode material. 5% SO_2 in nitrogen with 0.5 mol L^{-1} H_2SO_4 as supporting electrolyte. $t = 2$ h. $\omega = 1000$ rpm. $T = 30$ °C. U, cell voltage; E_S, specific energy consumption; ρ, space time yield.

was increased. Likewise, the comparison of Fig. 10 and Fig. 12 shows that the current drained by the three-dimensional anode is only three times higher than the value obtained with only the graphite support, despite the high specific surface area of the graphite felt. Then, the graphite felt improves the performance of the reactor but its surface area is not completely used, probably due to the contact resistance between the fibers of the felt or with the graphite support.

Figure 13 shows the change in sulfuric acid concentration as a function of current for GF-S4 under the conditions reported in Fig. 11. The gas volumetric flow rate was enlarged when the current increases in order to ensure that the reactant is in excess. The dashed line in Fig. 13 accounts for the gas volumetric flow rate and the number at each point represents the conversion of sulfur dioxide. Comparing Fig. 11 and Fig. 13 it can be seen that using a three-dimensional rotating cylindrical anode with a two phase flow induced by centrifugal force, it was possible to oxidize sulfur dioxide to sulfuric acid with current efficiencies near 100%.

Figure 14 reports on the figures of merit of the reactor as a function of the macrokinetic current density, i_b, defined as the ratio between the current and the external surface area of the three-dimensional structure. The data shown in Fig. 14 correspond to the experiments with anode potentials lower than 1.5 V in order to avoid oxygen evolution as a side reaction. As expected, cell voltage and space time yield increase with the current. Figure 14 also suggests that a macrokinetic current density of 100 mA cm^{-2} can be adopted for the operation of the reactor due to the high value of space time yield, 7.58 kg m^{-3} h^{-1} with a specific energy consumption of 2.86 kWh kg^{-1}, both related to sulfuric acid production. For these conditions, the average value of cell voltage was 5.18 V with 99.4% current efficiency and 91% for the conversion of sulfur dioxide. Similar values were reported for a batch reactor with a three-dimensional anode of a platinum expanded mesh by Tezcan Ün *et al.*[21]

CONCLUSIONS

- Conversion of sulfur dioxide can be performed either at the anode or at the cathode of an electrochemical reactor to obtain sulfuric acid and colloidal sulfur, respectively.

- Controlling the anode potential at values lower than 1.5 V against saturated calomel electrode, the main anodic reaction at a graphite electrode is the formation of sulfuric acid. Likewise, −0.7 V as cathodic potential represents an appropriate value for the production of colloidal sulfur using a stainless steel cathode. Thereby, the main products obtained at both electrodes have commercial value.
- A divided electrochemical reactor must be used in order to avoid the deactivation of the anode by the elemental sulfur cathodically produced. Microporous PVC was an appropriate separator.
- It is convenient to remove the elemental sulfur covering the cathode to maintain the current at a high value, which can be achieved by using either a scrapper or by hydrogen evolution at the cathode. This last alternative is counteracted by the decrease in current efficiency for the production of colloidal sulfur.
- An electrochemical reactor with a rotating cylinder electrode working either as anode or cathode showed an appropriate performance for the conversion of sulfur dioxide into useful chemicals.

ACKNOWLEDGEMENTS

This work was supported by the Agencia Nacional de Promoción Científica y Tecnológica (ANPCyT), Consejo Nacional de Investigaciones Científicas y Técnicas (CONICET) and Universidad Nacional del Litoral (UNL) of Argentina.

REFERENCES

1 Capone M, Sulfur removal and recovery, in *Encyclopedia of Chemical Technology*, ed. by Kirk RE and Othmer DF. John Wiley & Sons, New York, pp. 209–218 (1991).
2 Castro-González JA, Rivas-Penney CR, Durán-Moreno A and Durán de Bazúa C, Eliminación de óxidos de azufre de corrientes gaseosas: Estado del arte. *Tecnol Ciencia Ed (IMIQ)* **16**:89–100 (2001).
3 Kuhn AT, Electrochemical methods for SO_2 flue gas treatment. *J Appl Electrochem* **1**:41–44 (1971).
4 Sohm JC, Procédés électrochimiques de désulfurization des fumées. *Rev Gen Electr* **84**:305–314 (1975).
5 Kreysa G, Bisang JM, Kochanek W and Linzbach G, Fundamental studies on a new concept of flue gas desulphurization. *J Appl Electrochem* **15**:639–647 (1985).
6 Bakir Öğütveren Ü, Electrochemical processes for gaseous sulfur oxides (SO and SO_x) removal, in *Encyclopedia of Applied Electrochemistry*, ed. by Kreysa G, Ota K-i and Savinell RF. Springer, New York, pp. 543–548 (2014).
7 Oloman C, The preparation of dithionites by the electrolytic reduction of sulfur dioxide in water. *J Electrochem Soc* **117**:1604–1609 (1970).
8 Oloman C, Lee B and Leyten W, Electrosynthesis of sodium dithionite in a trickle-bed reactor. *Can J Chem Eng* **68**:1004–1009 (1990).
9 Scott K, Taama W and Cheng H, Towards an electrochemical process for recovering sulphur dioxide. *Chem Eng J* **73**:101–111 (1999).
10 Scott K and Taama WM, An investigation of anode materials in the anodic oxidation of sulphur dioxide in sulphuric acid solutions. *Electrochim Acta* **44**:3421–3427 (1999).
11 Struck BD, Schütz GH and Van Velzen D, Cathodic hydrogen evolution in thermochemical–electrochemical hybrid cycles, in *Electrochemical Hydrogen Technologies: Electrochemical Production and Combustion of Hydrogen*, ed. by Wendt H. Elsevier, Amsterdam, pp. 301–343 (1990).
12 Jomard F, Feraud JP and Caire JP, Numerical modeling for preliminary design of the hydrogen production electrolyzer in the Westinghouse hybrid cycle. *Int J Hydrogen Energy* **33**:1142–1152 (2008).
13 Mishra KK and Cooper WC, Electrochemical aspects of the direct electrowinning copper from sulfuric acid leach solutions in the presence of iron using gas sparging, in *Anodes for Electrowinning AIME Annual Meeting*, ed. by Robinson DJ and James SE. The Metallurgical Society of AIME, Los Angeles, California, pp. 13–36 (1984).
14 Samec Z and Weber J, Study of the oxidation of SO_2 dissolved in 0.5 M H_2SO_4 on a gold electrode – II. A rotating disc electrode. *Electrochim Acta* **20**:413–419 (1975).
15 Morris HE, Lacombe RE and Lane WH, Quantitative determination of elemental sulfur in aromatic hydrocarbons. *Anal Chem* **20**:1037–1039 (1948).
16 Kelsall GH and Thompson I, Redox chemistry of H_2S oxidation in the British Gas Stretford Process Part I: Thermodynamics of sulphur–water systems at 298 K. *J Appl Electrochem* **23**:279–286 (1993).
17 Feigl F and Anger V, *Spot Tests in Inorganic Analysis*. Elsevier, Amsterdam, pp. 437–438 (1972).
18 Kreysa G, Jüttner K and Bisang JM, Cylindrical three-dimensional electrodes under limiting current conditions. *J Appl Electrochem* **23**:707–714 (1993).
19 González Pérez O and Bisang JM, Electrochemical synthesis of hydrogen peroxide with a three-dimensional rotating cylinder electrode. *J Chem Technol Biotechnol* **89**:528–535 (2014).
20 Jeffery GH, Bassett J, Mendham J and Denney RC, *Vogel's Textbook of Quantitative Chemical Analysis*. Longman, Harlow, pp. 269–272 (1989).
21 Tezcan Ün Ü, Koparal AS and Bakir Öğütveren Ü, Electrochemical desulfurization of waste gases in a batch reactor. *J Environ Eng* **133**:13–19 (2007).

